

Electronic Supplementary Information

3D Binder-Free Cu₂O@Cu Nanoneedle Arrays for High-Performance Asymmetric Supercapacitors

Chaoqun Dong,^a Yan Wang,^b Junling Xu,^c Guanhua Cheng,^a Wanfeng Yang,^a Tianyi Kou,^a Zhonghua Zhang^{a*}, and Yi Ding^{a*}

^a Key Laboratory for Liquid-Solid Structure Evolution and Processing of Materials (Ministry of Education), School of Materials Science and Engineering, Shandong University, Jingshi Road 17923, Jinan 250061, P.R. China

^b School of Materials Science and Engineering, University of Jinan, No. 336, West Road of Nan Xinzhuang, Jinan 250022, P.R. China

^c Department of Electronic Engineering, The Chinese University of Hong Kong, New Territories, Hong Kong, P.R. China

E-mail: zh_zhang@sdu.edu.cn; yding@sdu.edu.cn

Experimental

Anodization of Cu foam and preparation of nanostructured Cu

The nanostructured Cu materials (nanostructuring of the skeleton surface of Cu foam) were prepared by a unique electrochemistry device in which a slice of clean Cu foam (120 pores per inch, 98% porosity, and ~ 1.0 mm thick) serviced as the anode electrode and a graphite plate as the cathode electrode, as shown in Scheme 1. The two parallel electrodes both with a working area of about 2.0 cm × 2.0 cm were immersed into a 0.4 M H₂C₂O₄ solution. The experiments were carried out at a constant potential of 12 V for 10 min. One possible reaction principle involved during this experiment is illustrated in Scheme1. By the effect of the extra power supply, Cu²⁺ ions which are formed in the anode combine C₂O₄²⁻ to form CuC₂O₄ precipitates in electrolyte, leaving pores on the surface of anode. At the same time, H⁺ ions attain electrons to form H₂ in the electrolyte near the cathode.

Synthesis of Cu₂O@Cu nanoneedle arrays electrode

The synthetic procedure of the Cu₂O@Cu nanoneedle arrays electrode was executed in a potentiostat (CHI 660E) with a three-electrode configuration, in which the as-prepared nanostructured Cu foam acted as the working electrode, a Pt foil (1cm×1cm) was used as the counter electrode and an Ag/AgCl electrode served as the reference electrode. Cyclic voltammetry in the potential range from -0.3 to 0.3 V at the scan rate of 1 mV s⁻¹ was employed in a 1 M KOH aqueous solution to induce the in-situ growth of Cu₂O@Cu nanoneedle arrays on the skeleton surface of Cu foam.

Assembly of Cu₂O@Cu//AC asymmetric supercapacitor

For the asymmetric supercapacitor, the as-prepared $\text{Cu}_2\text{O}@Cu$ electrode was used for the positive electrode and the active carbon (AC) acted as the negative electrode. The AC electrode was prepared according to the following procedures. Firstly, AC (TF-B520) was mixed with TIMCAL SUPER C45 conductive carbon black and polyvinylidene fluoride (PVDF), and their mass ratio was 8:1:1. Appropriate N-methyl pyrrolidone was added into the mixture as a solvent to make a slurry which was coated onto a nickel foam. Finally, the as-prepared electrode was dried at 80°C for 5 h to remove the solvent. The as-prepared positive electrode and negative electrode were separated by a cellulose paper and were face-to-face placed into an encapsulation, in which the 1 M KOH solution was added as the electrolyte.

Materials characterization

The phase formation of the as-synthesized samples was characterized using X-ray diffraction (XRD, Rigaku D/max-rB) with Cu $K\alpha$ radiation. Scanning electron microscope (SEM, Quanta FEG 250) was employed to observe the surface morphology and structure of the $\text{Cu}_2\text{O}@Cu$ electrode. Nitrogen adsorption/desorption isotherms were measured at 77 K with a V-Sorb 2800P Surface Area and Pore Size Analyzer. The specific surface area was calculated using the Brunauer-Emmett-Teller (BET) method. The pore size distribution was obtained by Barrett-Joyner-Halenda (BJH) method. The resistivity of Cu foam and the $\text{Cu}_2\text{O}@Cu$ electrode was measured by a constant current four-electrode method, and was recorded every 2 s by a computer connected to the measurement system.

Electrochemical measurements

The electrochemical properties of the $\text{Cu}_2\text{O}@Cu$ electrode were measured by the CHI

660E potentiostat in a cell with using a conventional three-electrode configuration. The Pt foil was used as the counter electrode and an Ag/AgCl electrode was used as the reference electrode. All electrochemical measurements of the Cu₂O@Cu//AC asymmetric supercapacitor were performed by the CHI 660E potentiostat with a two-electrode mode. All electrochemical measurements were carried out in the 1 M KOH aqueous solution at room temperature. The electrochemical impedance spectroscopy (EIS) of both the Cu₂O@Cu electrode and the Cu₂O@Cu//AC asymmetric supercapacitor was performed in a frequency range from 0.01 Hz to 100 kHz with a 5 mV amplitude at open circuit potential.

Calculations:

The specific capacitance, one of the most important parameters for characterizing the electrochemical performance of supercapacitors, can be calculated from the CVs according to the following equation:¹

$$C_m = \frac{1}{mv(V_c - V_a)} \int_{V_a}^{V_c} I(V) dV \quad (1)$$

Where C_m is the specific capacitance (F g⁻¹), m is the mass of electroactive materials in the electrode (g), v is the potential scan rate (mV s⁻¹), V_c and V_a represent the highest and lowest voltages (V), respectively, $I(V)$ is the response current density (A), and V is the potential (V).

The theoretical pseudocapitance of metal oxide can be calculated as:²

$$C = \frac{n \times F}{M \times V} \quad (2)$$

where n is the mean number of the electrons transferred in the redox reaction, F is the Faraday constant, M is the molar mass of the metal oxide and V is the operating voltage window. Then, we obtained the theoretical capacitance of Cu_2O : $(2 \times 96485.3383 / 0.6 / 143.091) \text{ F g}^{-1} = 2247.6 \text{ F g}^{-1}$.

The specific capacitance of the electrode can also be calculated from galvanostatic charge-discharge curves by the following formula:^{3, 4}

$$C_m = \frac{I \times \Delta t}{m \times \Delta V} \quad (3)$$

where C_m is the specific capacitance (F g^{-1}), I is the constant discharge current (A), Δt is the discharging time (s), m is the mass of Cu_2O (g), and ΔV is the discharging potential range (V).

The mass of Cu_2O was calculated by means of the following steps. Firstly, the mass of the completely clean and dried $\text{Cu}_2\text{O}@Cu$ electrode, named m_1 , was weighed by electronic balance with an accuracy of 0.0001 g. Secondly, this electrode was immersed into a N_2 -saturated 0.1 M HCl solution about 10 min until no obvious colour change occurred. During this step, the Cu_2O layer was removed. The mass of the Cu foam, named m_2 , was weighed again after careful washing with highly pure de-ionized water and complete drying. Finally, the mass of Cu_2O attached on Cu foam was calculated ($m_1 - m_2$). The mass loading of Cu_2O nanoneedles per area was 1.72 mg cm^{-2} .

In order to obtain an asymmetric supercapacitor with high electrochemical performance, the charge balance between the two electrodes should follow the relationship $q_+ = q_-$. The q is the charge stored by electrode, which can be calculated by

the equation:⁵

$$q = C_s \times \Delta E \times m \quad (4)$$

where C_s is the specific capacitance ($F\ g^{-1}$), ΔE is the potential range of the charge-discharge process (V), m is the mass loading of the electroactive material on the electrode (g). According to equation (4), the ideal mass ratio of electroactive material on the positive and negative electrode in a asymmetric supercapacitor (m_+/m_-) can be calculated using the formula:⁵

$$\frac{m_+}{m_-} = \frac{c_- \times \Delta E_-}{c_+ \times \Delta E_+} \quad (5)$$

The specific capacitance of $Cu_2O@Cu$ positive electrode and AC negative electrode calculated from the CV curves at the scan rate of $5\ mV\ s^{-1}$ are 681.2 and 113.9 $F\ g^{-1}$, respectively. Based on the analysis above, the ideal mass ratio of m_+/m_- of the asymmetric supercapacitor should be 0.33 in the present work. The total mass of the positive electrode in our experiments was $1.72\ mg\ cm^{-2}$, and that on the negative electrode was $4.92\ mg\ cm^{-2}$. This value was close to the calculated ideal mass ratio of 0.33.

The energy densities and corresponding power densities were calculated from the following equations:^{4, 6}

$$E = \frac{1}{2} C_m (\Delta V)^2 \quad (6)$$

$$P = \frac{E}{\Delta t} \quad (7)$$

where E is the energy density, C_m is the capacitance of the capacitor, ΔV is the operating potential window, P is the power density, and Δt is the discharge time.

Supplementary Figures (Fig. S1-S9)

Supplementary Videos (Video S1-S3)

Supplementary Figures:

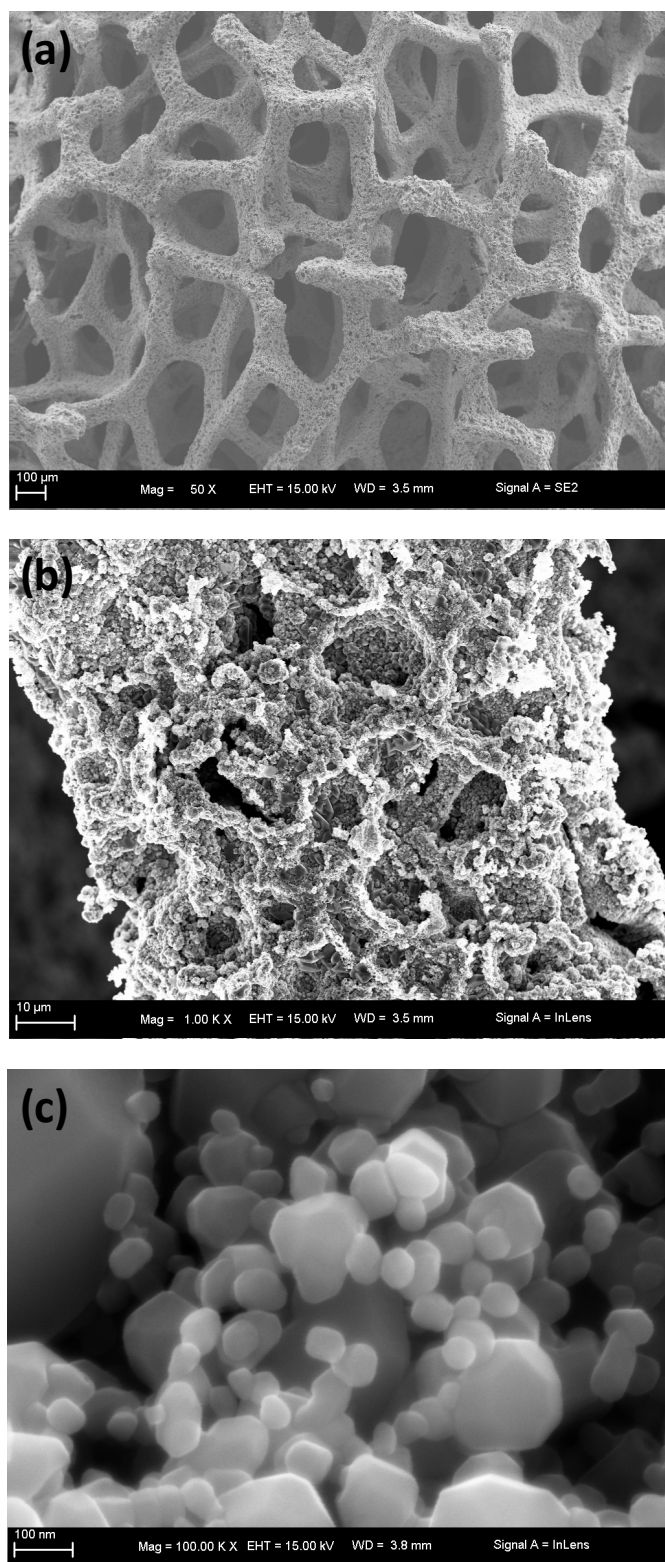


Figure S1. SEM images of the Cu foam after processing in the $\text{H}_2\text{C}_2\text{O}_4$ solution at different magnifications.

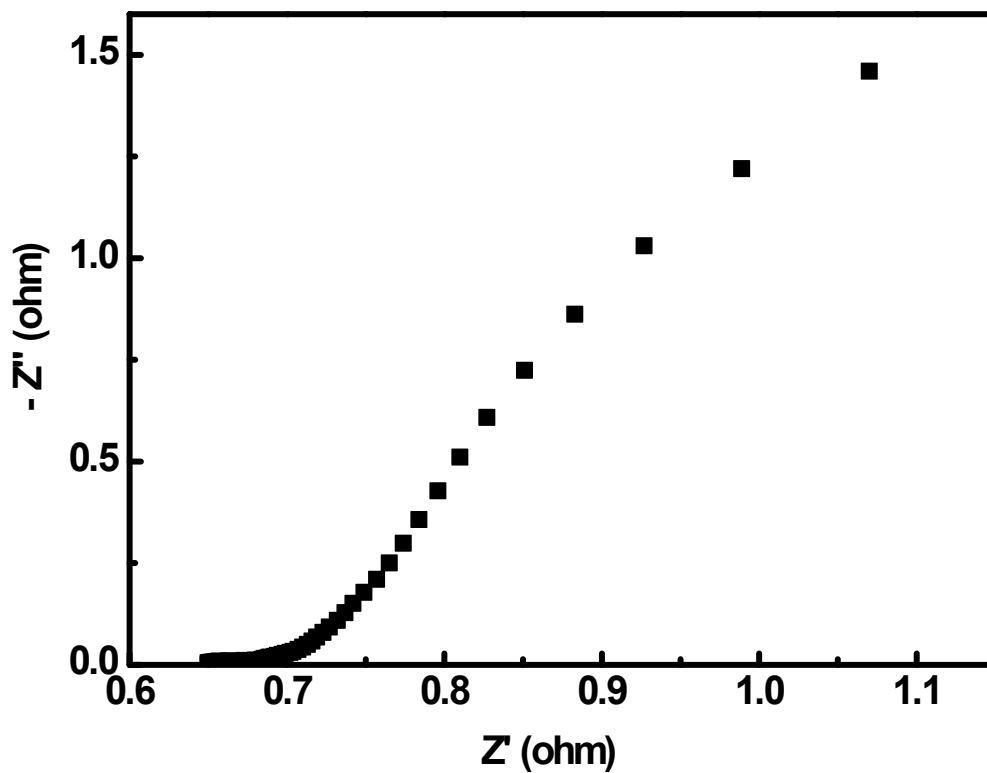


Figure S2. Nyquist diagram of the $\text{Cu}_2\text{O}@\text{Cu}$ electrode carried out in a frequency range from 0.01 Hz to 100 kHz with a 5 mV amplitude at open circuit potential.

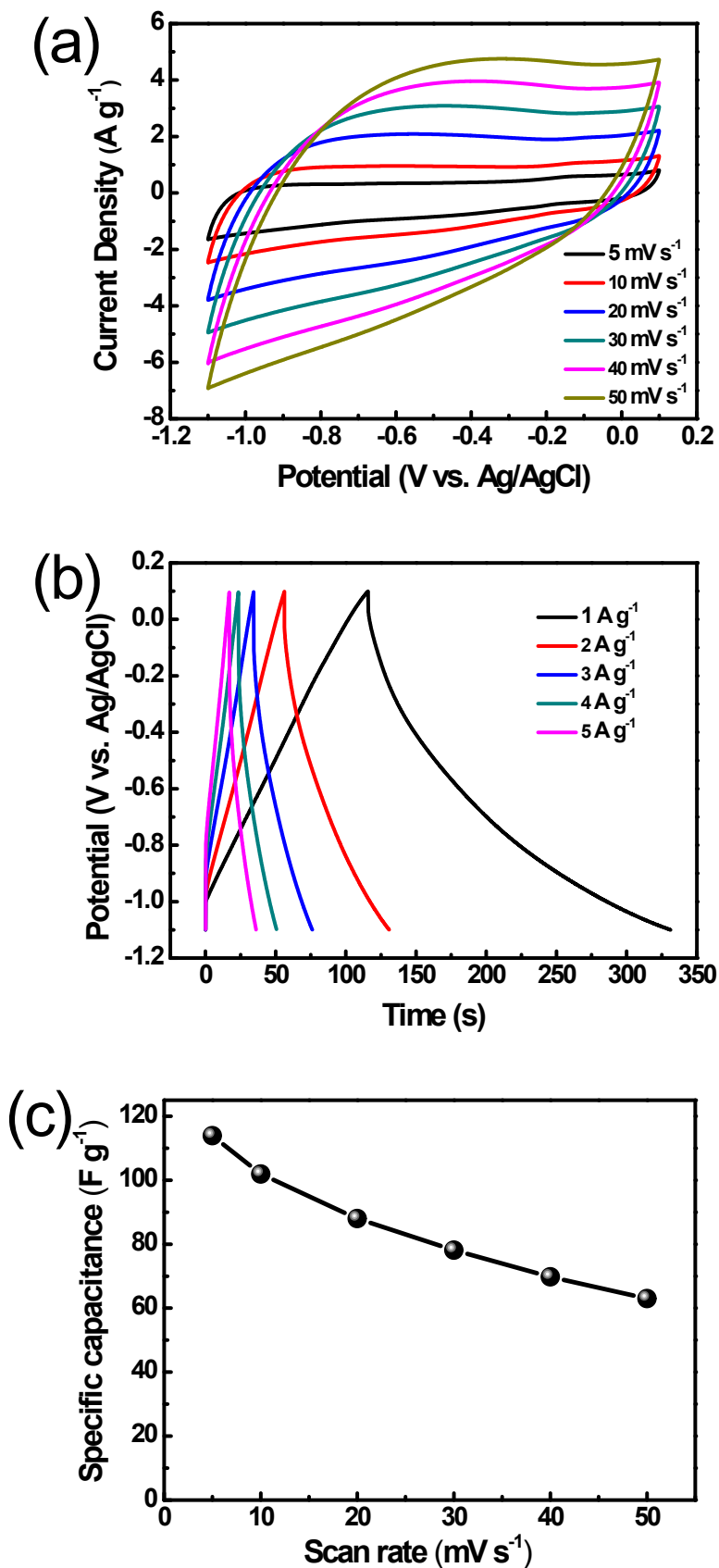


Figure S3. Electrochemical characterization of the AC electrode. (a) CV curves of the AC electrode at various scan rates (ranging from 5 to 50 mV s^{-1}). (b)

Galvanostatic charge-discharge curves of the electrode at various current densities (ranging from 1 to 5 A g⁻¹). (c) Specific capacitance of the AC electrode as a function of scan rate based on the CVs. It should be noted that the CVs of the AC electrode appear nearly rectangular, and no obvious redox peaks can be observed. The shape of galvanostatic charge-discharge curves is symmetrical, indicating a typical feature of an electric double-layer capacitance.

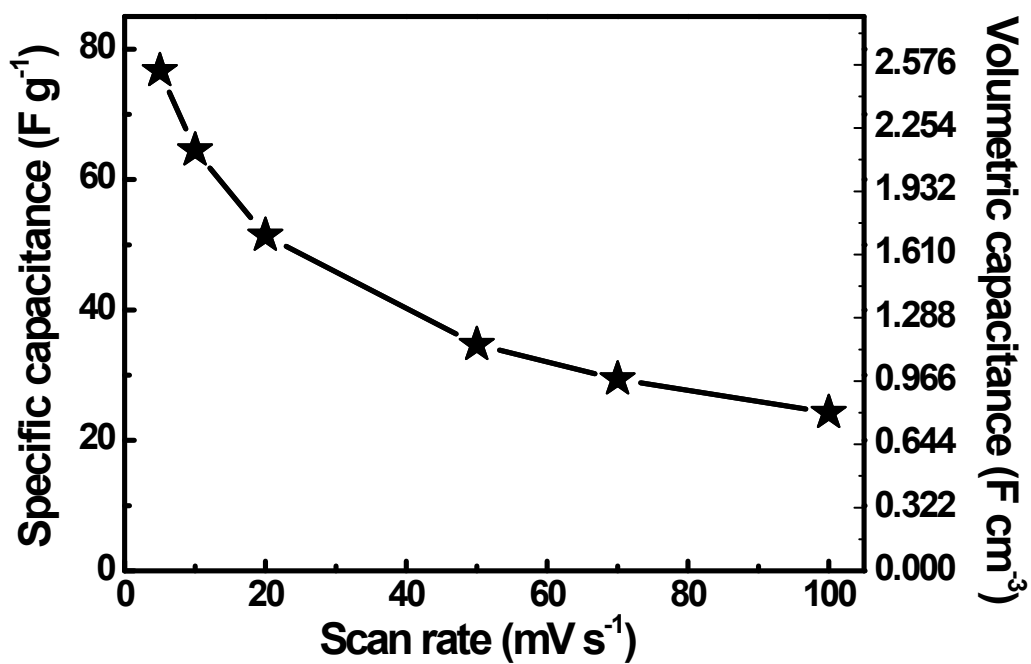


Figure S4. Specific capacitance and volumetric capacitance of the Cu₂O@Cu//AC asymmetric capacitor as a function of scan rate based on the CV curves.

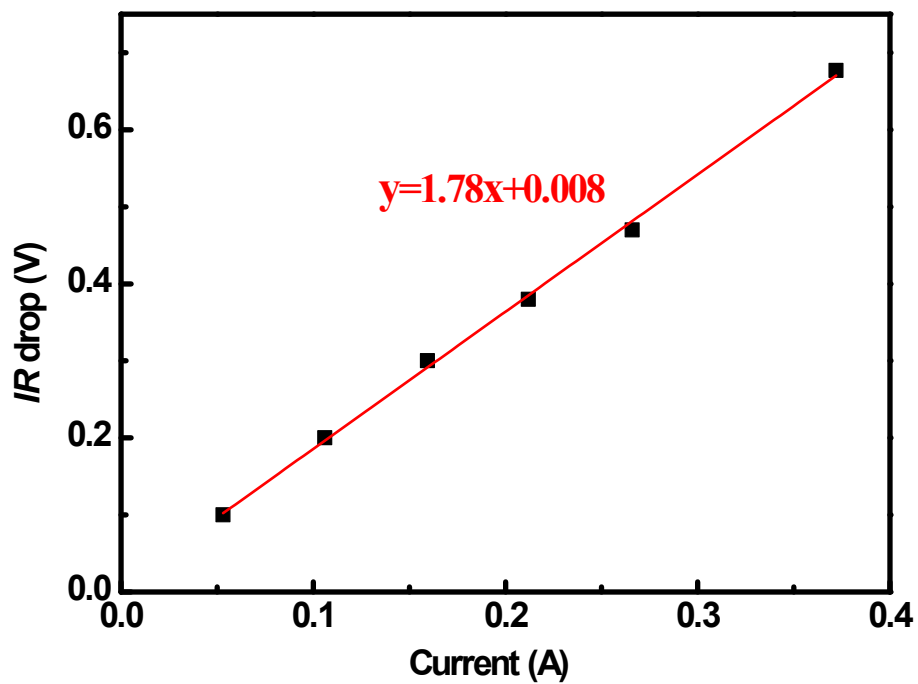


Figure S5. Variation of IR drop with the total change in current of the charge-discharge measurement.

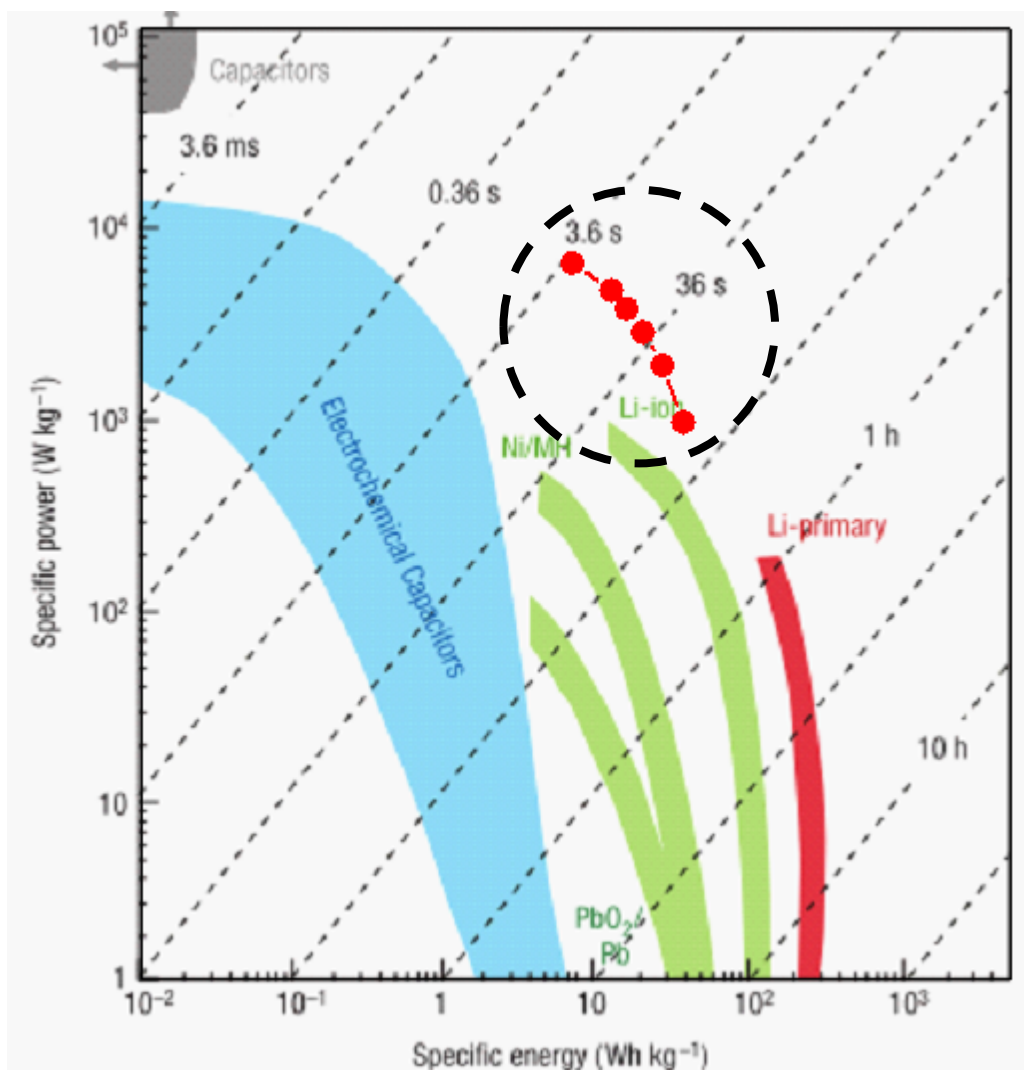


Figure S6. The Ragone plot of the $\text{Cu}_2\text{O}@\text{Cu}/\text{AC}$ asymmetric supercapacitor (red solid circles highlighted by a black dotted circle), along with various electrical energy storage devices. The plot was made based on the Figure 1 in the literature by Prof. P. Simon.⁷ Compared with other energy storage devices, our $\text{Cu}_2\text{O}@\text{Cu}/\text{AC}$ supercapacitors present remarkable energy density and high power density.

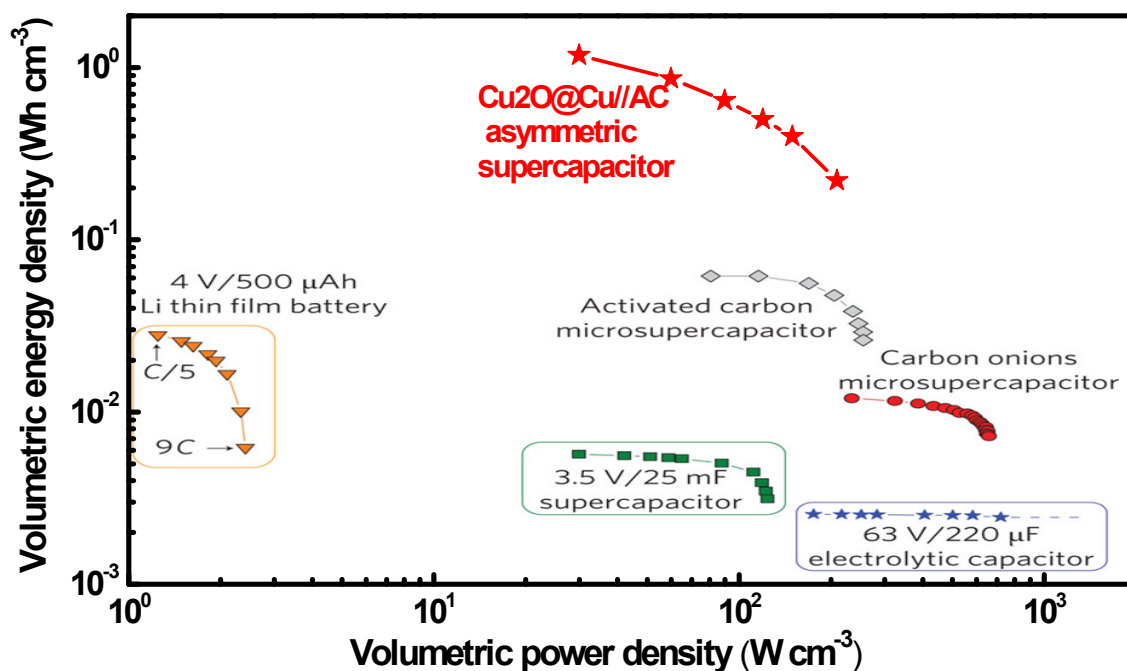


Figure S7. The Ragone plot of the $\text{Cu}_2\text{O}@\text{Cu}//\text{AC}$ asymmetric supercapacitor (red solid stars), along with typical literature results for supercapacitors and batteries. The plot was made based on Figure 4 in the article by Prof. P. Simon and co-workers.⁸ The volumetric energy densities of the $\text{Cu}_2\text{O}@\text{Cu}//\text{AC}$ asymmetric supercapacitor are 0.22, 0.40, 0.50, 0.64, 0.86, and 1.18 Wh cm^{-3} at various power densities of 209.16, 149.40, 119.52, 89.64, 59.76, 29.88 W cm^{-3} respectively.

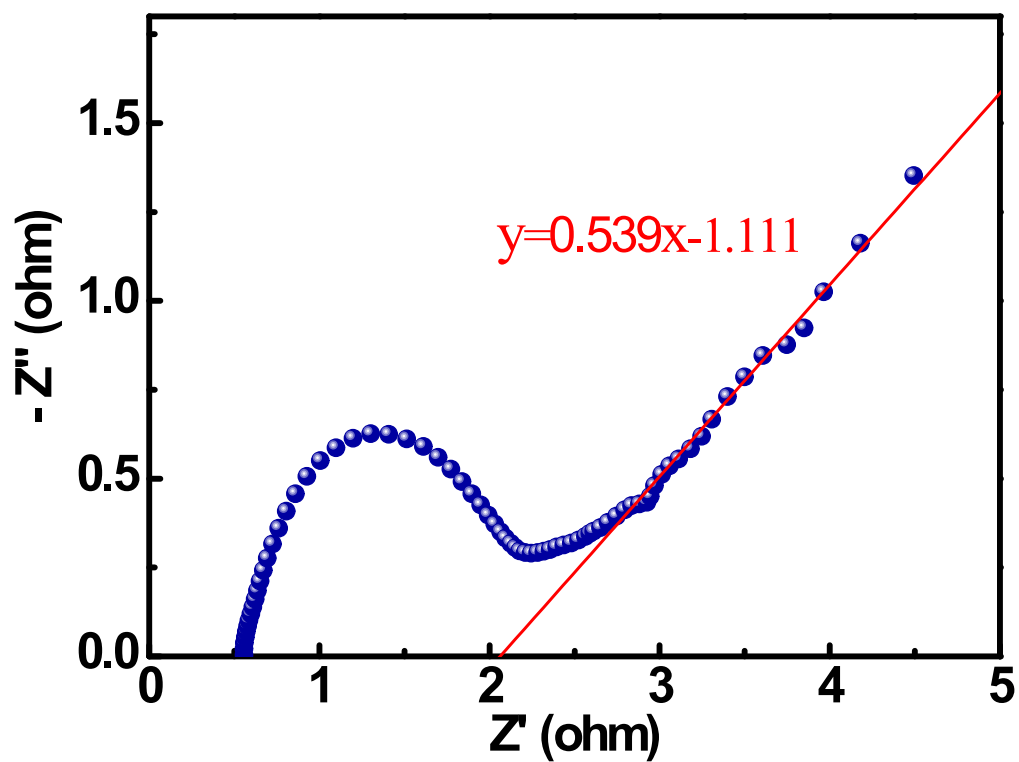


Figure S8. Linear fitting for the linear section in the Nyquist plot low-frequency region of the $\text{Cu}_2\text{O}@Cu//\text{AC}$ asymmetric supercapacitor.

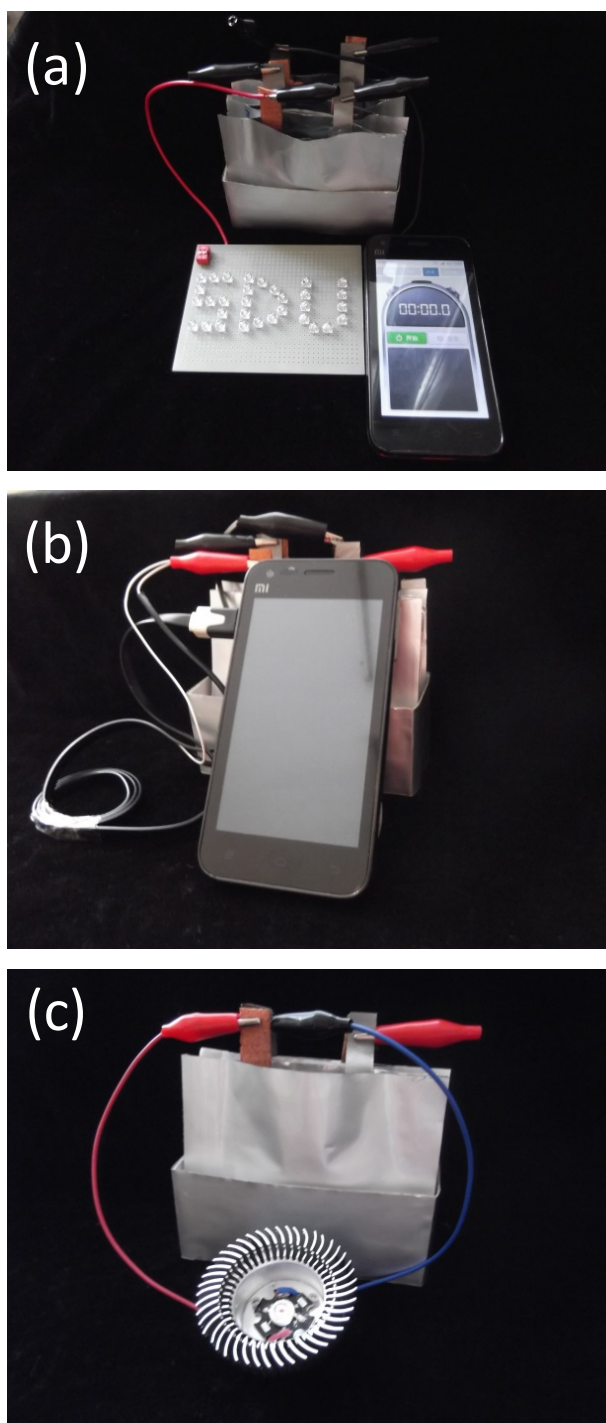


Figure S9. Digital photographs of line connection between the $\text{Cu}_2\text{O}@\text{Cu}/\text{AC}$ asymmetric supercapacitors and demonstration devices. (a) Four supercapacitors in series and a 32-LEDs displayer. (b) Two supercapacitors and a mobile phone awaiting for charging. (c) Two supercapacitors and a 1W yellow LED.

Supplementary Videos:

Video S1: Video showing that four supercapacitors in series can light up a 32-LEDs displayer.

Video S2: Video showing that two supecapacitors in series are charging a mobile phone.

Video S3: Video showing a 1W yellow LED powered by two supercapacitors in series.

Notes and References

1. Z. Fan, J. Yan, T. Wei, L. Zhi, G. Ning, T. Li, F. Wei, *Adv. Funct. Mater.*, 2011, **21**, 2366 – 2375.
2. M. Zhi, C. Xiang, J. Li, M. Li, N. Wu, *Nanoscale*, 2013, **5**, 72 – 88.
3. X. Yu, B. Lu, Z. Xu, *Adv. Mater.*, 2014, **26**, 1044 – 1051.
4. Q. Lu, M. W. Lattanzi, Y. Chen, X. Kou, W. Li, X. Fan, K. M. Unruh, J. G. Chen, J. Q. Xiao, *Angew. Chem. Int. Ed.*, 2011, **50**, 6847 – 6850.
5. J. Yan, Z. Fan, W. Sun, G. Ning, T. Wei, Q. Zhang, R. Zhang, L. Zhi, F. Wei, *Adv. Funct. Mater.*, 2012, **22**, 2632 – 2641.
6. X. Wang, A. Sumboja, M. Lin, J. Yan, P. S. Lee, *Nanoscale*, 2012, **4**, 7266 – 7272.
7. P. Simon, Y. Gogotsi, *Nat. Mater.*, 2008, **7**, 845 – 854.
8. D. Pech, M. Brunet, H. Durou, P. Huang, V. Mochalin, Y. Gogotsi, P.-L. Taberna, P. Simon, *Nat. Nanotechnol.*, 2010, **5**, 651 – 654.